The Synthesis of $[Ru_5C(CO)_{15}]$ by the Carbonylation of $[Ru_6C(CO)_{17}]$ and the Reactions of the Pentanuclear Cluster with a Variety of Small Molecules: the *X*-Ray Structure Analyses of $[Ru_5C(CO)_{15}]$, $[Ru_5C(CO)_{15}(MeCN)]$, $[Ru_5C(CO)_{14}(PPh_3)]$, $[Ru_5C(CO)_{13}(PPh_3)_2]$, and $[Ru_5(\mu\text{-}H)_2C(CO)_{12}\{Ph_2P(CH_2)_2PPh_2\}]$ †

Brian F. G. Johnson, Jack Lewis,* J. Nicola Nicholls, José Puga, Paul R. Raithby, and Maria J. Rosales
University Chemical Laboratory, Lensfield Road, Cambridge CB2 1EW
Mary McPartlin
Chemistry Department, The Polytechnic of North London, London N7 8DB
William Clegg
Anorganisch-Chemisches Institut der Universität, Tammannstrasse 4, D-3400 Göttingen, West Germany

The hexaruthenium cluster $[Ru_6C(CO)_{17}]$ reacts with CO at 70 °C and 80 atm to produce $[Ru_5C(CO)_{15}]$ (1) and $[Ru(CO)_5]$. Complex (1) crystallises in space group $P2_1/c$ with a = 16.448(3), b = 14.274(2), c = 20.834(4) Å, β = 91.36(2)°, and Z = 8. The structure was found to be isomorphous with the analogue $[Os_5C(CO)_{15}]$, and was refined to R = 0.051 for 3 256 diffractometer data. The five Ru atoms adopt a square-pyramidal geometry with an exposed carbido-atom lying 0.11(2) Å beneath the basal plane. Reaction of complex (1) with the nitrogen-donor ligand MeCN yields the adduct $[Ru_5C(CO)_{15}(MeCN)]$ (2) which exhibits a bridged butterfly arrangement of metal atoms with a central carbido-atom. The complex crystallises in space group $P2_1/n$ with a = 14.116(6), b = 18.167(7), c = 10.276(4) Å, β = 95.14(3)°, and Z = 4; the structure was solved by direct methods and difference techniques and refined to R = 0.047 for 1 604 diffractometer data. Reactions of complex (1) with tertiary phosphine ligands PR_3 [R = Ph (3) or $MePh_2$(4)] or $Ph_2P(CH_2)_nPPh_2$ [n = 1 (5) or 2 (6)] produce the substituted complexes $[Ru_5C(CO)_{15-m}(PR_3)_m]$ [m = 1 (3a, 4a), 2 (3b, 4b), or 3 (3c, 4c)] or $[Ru_5C(CO)_{13}\{Ph_2P(CH_2)_nPPh_2\}]$ [n = 1 (5) or 2 (6)]. The structures of these complexes are closely related to that of (1). Complex (3a) crystallises in space group Pn with a = 9.953(2), b = 12.247(2), c = 14.703(3) Å, β = 91.23(2)°, and Z = 2, (3b) in space group $P2_1/c$ with a = 15.923(4), b = 12.494(3), c = 25.210(7) Å, β = 93.28(2)°, and Z = 4. Both structures were solved by a combination of direct methods and Fourier techniques and were refined to R = 0.021 for 3 305 reflections (3a) and R = 0.039 for 4 127 reflections (3b), respectively. Hydrogenation of (6) gives the dihydro-complex $[Ru_5(\mu\text{-}H)_2C(CO)_{12}\{Ph_2P(CH_2)_2Ph_2\}]$ which crystallises in space group $P2_1$ with a = 12.210(4), b = 18.602(6), c = 18.409(6) Å, β = 97.63(2)°, and Z = 4. The structure was solved using the same techniques as the other complexes and refined to R = 0.064 for 3 510 diffractometer data. Treatment of complex (1) with halide ions gives the anionic clusters $[Ru_5C(CO)_{15}X]^-$ (X = F, Cl, Br, or I) whose structures are similar to that of (2). Protonation of these anions gives the monohydrido-clusters $[Ru_5H(C)(CO)_{15}X]$. With Cl_2 and Br_2 complex (1) undergoes fragmentation to give dimers $[Ru_2(CO)_6X_4]$ (X = Cl or Br); in contrast, reaction with I_2 gives $[Ru_5C(CO)_{15}I_2]$.

In recent years there has been increasing support [1] for the view that an important step in the Fischer–Tropsch hydrogenation of carbon monoxide to produce alkanes involves C–O bond cleavage and the production of carbido-metal intermediates. Fundamental to our understanding of this reaction will be an evaluation of the mechanisms by which such carbido-intermediates may be produced and also the type of reactivity that such species exhibit. Several years ago we reported [2] the preparation of the hexanuclear carbido-cluster $[Ru_6C(CO)_{17}]$ from the pyrolysis of $[Ru_3(CO)_{12}]$ in a sealed tube or on heating in an appropriate solvent. An *X*-ray structural analysis of this compound [3] and that of the closely related derivative $[Ru_6C(CO)_{14}(C_6H_3Me_3)]$ [4] clearly demonstrated that the carbido-atom is encapsulated within an Ru_6 octahedron and as such is apparently protected from attack by incoming substrates (see Figure 1). It was also established that the reaction proceeded according to equation (i) and that the source of this carbido-atom was carbon monoxide.

$$2\,[Ru_3(CO)_{12}] \longrightarrow [Ru_6C(CO)_{17}] + 5\,CO + CO_2 \qquad \text{(i)}$$

In this paper we report the synthesis, structure, and some aspects of the reactivity of the pentanuclear carbido-cluster $[Ru_5C(CO)_{15}]$ which has been obtained in high yields by the direct carbonylation of $[Ru_6C(CO)_{17}]$. A preliminary report of some of this work has appeared.[5]

Results and Discussion

Preparation of $[Ru_5C(CO)_{15}]$ *by the Carbonylation of* $[Ru_6C(CO)_{17}]$.—The hexanuclear cluster $[Ru_6C(CO)_{17}]$ reacts

---

† μ_5-Carbido-*cyclo*-pentakis(tricarbonylruthenium)(8*Ru–Ru*), 1,3-μ-acetonitriletricarbonylruthenio-μ_5-carbido-*cyclo*-tetrakis(tricarbonylruthenium)(7*Ru–Ru*); μ_5-carbido-1,1,1,2,2,2,3,3,3,4,4,4,5,5-tetradecacarbonyl-5-triphenylphosphine-, μ_5-carbido-1,1,1,2,2,2,3,-3,4,4,4,5,5-tridecacarbonyl-3,5-bis(triphenylphosphine)-, and 5-[1′,2′-bis(diphenylphosphino)ethane-*PP*′]-μ_5-carbido-2,3;3,4-di-μ-carbonyl-1,1,1,2,2,3,3,4,4,5-decacarbonyl-1,5;2,5-di-μ-hydrido-*cyclo*-pentaruthenium(8*Ru–Ru*).

Supplementary data available (No. SUP 23478, 129 pp.): thermal parameters, H-atom co-ordinates, complete bond parameters, structure factors. See Notices to Authors No. 7, *J. Chem. Soc., Dalton Trans.*, 1981, Index issue.

Non-S.I. units employed: atm = 101 325 Pa, eV ≈ 1.60×10^{-19} J.

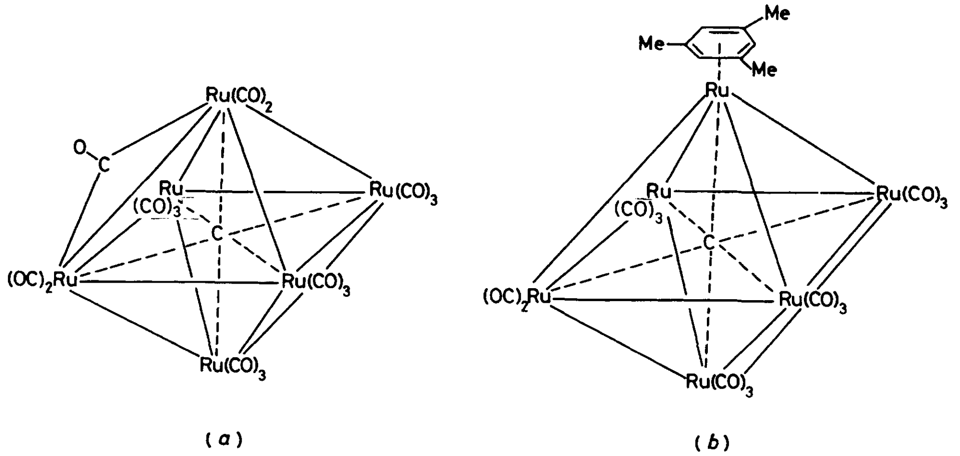

(a) (b)

Figure 1. The structures of (a) $[Ru_6C(CO)_{17}]$ and (b) $[Ru_6C(CO)_{14}(C_6H_3Me_3)]$

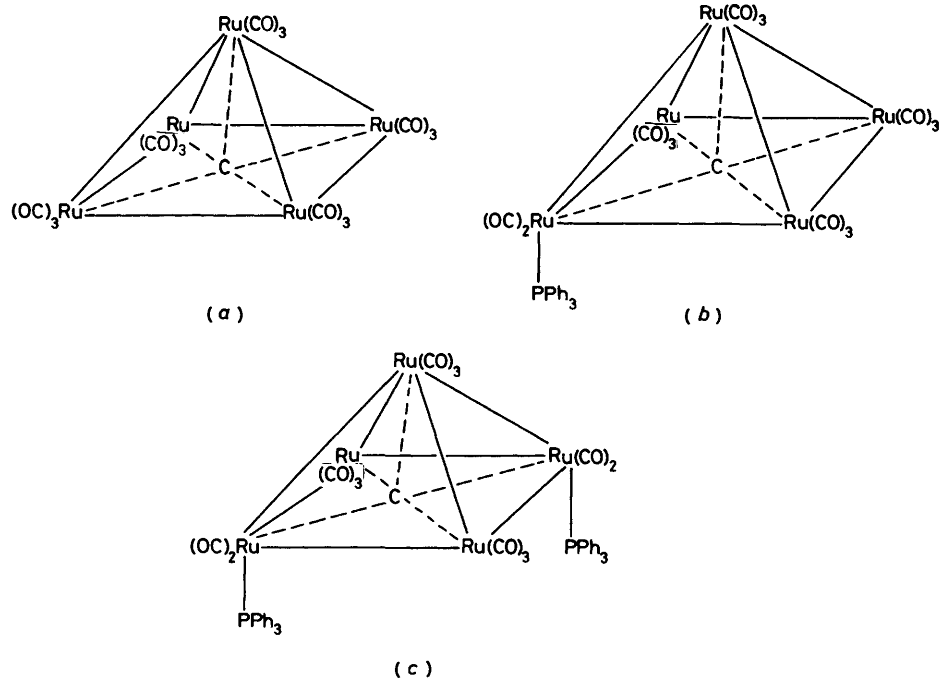

(a) (b)

(c)

Figure 2. Representations of the structures of (a) $[Ru_5C(CO)_{15}]$, (b) $[Ru_5C(CO)_{14}(PPh_3)]$, and (c) $[Ru_5C(CO)_{13}(PPh_3)_2]$

with CO under moderate conditions to produce quantitative amounts of the pentanuclear cluster $[Ru_5C(CO)_{15}]$ (1) and $[Ru(CO)_5]$ according to equation (ii). This is in contrast to the

$$[Ru_6C(CO)_{17}] \xrightarrow[70\ ^\circ C,\ 3\ h]{CO,\ 80\ atm} \underset{(1)}{[Ru_5C(CO)_{15}]} + [Ru(CO)_5] \quad (ii)$$

previously reported[6] route to this compound in which the tetranuclear hydride $[Ru_4H_4(CO)_{12}]$ was treated with ethylene to produce amongst a number of other products $[Ru_5C(CO)_{15}]$ in yields of *ca.* 1%. The mononuclear product of reaction (ii) was readily identified as ruthenium pentacarbonyl on the basis of its spectroscopic properties; this readily converts into $[Ru_3(CO)_{12}]$ which may be recycled according to equations (i) and (ii).

The related iron carbido-cluster $[Fe_5C(CO)_{15}]$ has been known for some considerable time[7] and was the first carbido-carbonyl cluster to be reported. We have previously reported[8] the osmium analogue, $[Os_5C(CO)_{15}]$, as a minor product of the pyrolysis of $[Os_3(CO)_{12}]$. The molecular structures of these two species have been determined by single-crystal *X*-ray analysis.[7,8] In each case the metal polyhedron consists of a square-pyramidal arrangement with the carbido-atom occupying a site slightly below the square basal plane. The similarity of the i.r. spectrum of $[Ru_5C(CO)_{15}]$ to that of the iron and osmium analogues led us to predict that the ruthenium compound would possess this same structure (Table 1). This has now been verified by single-crystal *X*-ray analysis (see below) [Figure 2(*a*)].

Some Reactions of $[Ru_5C(CO)_{15}]$.—The availability of $[Ru_5C(CO)_{15}]$ has led us to examine its chemistry in more detail. It is soluble in a variety of hydrocarbon and chlorin-

Table 1. Infrared carbonyl stretching frequencies [a]

	Complex	ν(CO)/cm^{-1}
(1)	$[Ru_5C(CO)_{15}]$ [b]	2 067vs, 2 034s, 2 015w
(2)	$[Ru_5C(CO)_{15}(MeCN)]$ [c]	2 106w, 2 067m (sh), 2 053s, 2 042m (sh), 2 021m (sh), 2 011m
(3a)	$[Ru_5C(CO)_{14}(PPh_3)]$ [b]	2 087w, 2 056s, 2 046m, 2 025s, 2 014m
(3b)	$[Ru_5C(CO)_{13}(PPh_3)_2]$	2 066w, 2 041s, 2 010s (br)
(4c)	$[Ru_5C(CO)_{12}(PMePh_2)_3]$	2 050m, 2 021s, 2 002vs, 1 980m
(6)	$[Ru_5C(CO)_{13}\{Ph_2P(CH_2)_2PPh_2\}]$	2 072m, 2 036m, 2 023s, 2 005m, 1 997m
(9)	$[Ru_5C(CO)_{15}Cl]^-$	2 091w, 2 057s, 2 042vs, 2 014s
(10)	$[Ru_5C(CO)_{15}Br]^-$	2 091w, 2 057s, 2 042vs, 2 015s
(11)	$[Ru_5C(CO)_{15}I]^-$	2 085w, 2 057s, 2 038vs, 2 012s
(9a)	$[Ru_5H(C)(CO)_{15}Cl]$	2 087s, 2 072 (sh), 2 069s, 2 059s, 2 028m (br)
(10a)	$[Ru_5H(C)(CO)_{15}Br]$	2 087s, 2 072 (sh), 2 069s, 2 059s, 2 028m (br)
(14)	$[Ru_5C(CO)_{15}I_2]$	2 106w, 2 077s (sh), 2 071vs, 2 067s (sh), 2 059m (sh), 2 033m
(7)	$[Ru_5H_2(C)(CO)_{12}\{Ph_2P(CH_2)_2PPh_2\}]$ [b]	2 066s, 2 029vs, 2 020s 2 004s, 1 837(2)

[a] In $CHCl_2$ unless otherwise stated. [b] In hexane. [c] In MeCN.

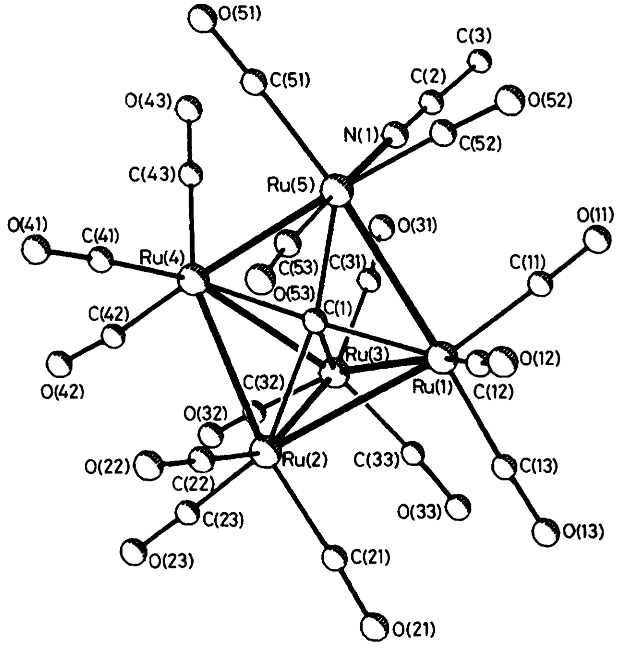

Figure 3. The molecular structure of $[Ru_5C(CO)_{15}(MeCN)]$ showing the atom-numbering scheme adopted

Table 2. Selected bond lengths (Å) and angles (°) for $[Ru_5C(CO)_{15}(MeCN)]$ (2)

Ru(1)-Ru(2)	2.886(3)	Ru(2)-Ru(3)	2.720(3)
Ru(1)-Ru(3)	2.888(3)	Ru(2)-Ru(4)	2.873(3)
Ru(1)-Ru(5)	2.873(3)	Ru(3)-Ru(4)	2.887(3)
Ru(1)-C(1)	1.968(17)	Ru(4)-Ru(5)	2.886(3)
Ru(2)-C(1)	2.076(18)	Ru(5)-N(1)	2.119(5)
Ru(3)-C(1)	2.068(18)	N(1)-C(2)	1.101(24)
Ru(4)-C(1)	1.961(17)	C(2)-C(3)	1.453(27)
Ru(5)-C(1)	2.158(18)		

Ru(2)-Ru(1)-Ru(3)	56.2(1)	Ru(1)-Ru(2)-Ru(3)	61.9(1)
Ru(2)-Ru(1)-Ru(5)	86.8(1)	Ru(1)-Ru(2)-Ru(4)	86.0(1)
Ru(3)-Ru(1)-Ru(5)	87.0(1)	Ru(3)-Ru(2)-Ru(4)	62.1(1)
Ru(1)-Ru(3)-Ru(2)	61.9(1)	Ru(2)-Ru(4)-Ru(3)	56.3(1)
Ru(1)-Ru(3)-Ru(4)	85.7(1)	Ru(2)-Ru(4)-Ru(5)	86.8(1)
Ru(2)-Ru(3)-Ru(4)	61.6(1)	Ru(3)-Ru(4)-Ru(5)	86.8(1)
Ru(1)-Ru(5)-Ru(4)	86.0(1)	Ru(1)-C(1)-Ru(2)	91.0(7)
Ru(2)-C(1)-Ru(4)	90.7(7)	Ru(1)-C(1)-Ru(3)	91.3(7)
Ru(2)-C(1)-Ru(5)	138.3(9)	Ru(2)-C(1)-Ru(3)	82.0(7)
Ru(3)-C(1)-Ru(5)	139.6(9)	Ru(1)-C(1)-Ru(4)	176.8(10)
Ru(4)-C(1)-Ru(5)	88.8(7)	Ru(5)-N(1)-C(2)	171.0(16)
		N(1)-C(2)-C(3)	177.5(21)

ated solvents to give stable red solutions, but in co-ordinating solvents such as acetonitrile or methanol an immediate reaction occurs giving adducts of the type $[Ru_5C(CO)_{15}(solv)]$ (solv = MeCN or MeOH). A similar reaction occurs with ethanol but at a much lower rate. By careful evaporation of solvent it has been possible to isolate the compound $[Ru_5C(CO)_{15}(MeCN)]$ (2) from solutions of $[Ru_5C(CO)_{15}]$ in MeCN. Under vacuum or on dissolution in chlorinated solvents such as dichloromethane the complex readily releases the acetonitrile molecule and reforms the parent molecule [equation (iii)]. The i.r. spectrum of this orange, crystalline material is more complicated than that of the parent molecule showing six rather than four bands in the ν(CO) region (Table 1). Overall, a shift to slightly lower frequencies (*ca.* 25 cm^{-1}) is also apparent. The structure of this new pentanuclear species has been established by *X*-ray analysis and is shown in Figure 3. Some selected bond lengths and bond angles are presented in Table 2. Essentially it consists of a butterfly of four ruthen-

$$\underset{(1)}{[Ru_5C(CO)_{15}]} + MeCN \rightleftharpoons \underset{(2)}{[Ru_5C(CO)_{15}(MeCN)]} \qquad (iii)$$

ium atoms with the two ' wing-tip ' atoms Ru(1) and Ru(4) bridged by this fifth ruthenium Ru(5). The carbido-atom resides within this polyhedron which corresponds to a distorted trigonal bipyramid, and may be regarded as semi-exposed being neither totally encapsulated as in $[Ru_6C(CO)_{17}]$ nor completely exposed as in $[Ru_5C(CO)_{15}]$ (1). The acetonitrile ligand is bonded to the bridging ruthenium atom, Ru(5), and the mechanism by which the compound is produced may be envisaged as a simple edge-break process directly from $[Ru_5C(CO)_{15}]$ (1) (Figure 4).

It may be argued that the ability of $[Ru_5C(CO)_{15}]$ (1) to act as an electron-pair acceptor stems initially from its inherent electron deficiency. Although the molecule may be regarded as electron-precise, in the sense that it is a 74-electron species and thereby apparently has sufficient electrons to form eight polyhedral edge bonds, because a connectivity of four is observed for the apical ruthenium atom and because it contains an interstitial carbon atom a more appropriate bond scheme is required. On the basis of the skeleton electron-pair theory [9] the clusters may be more appropriately regarded as electron deficient with $S = 7$ and, as such, may be described as *nido* octahedra. On this basis the site of nucleophilic attack is expected to be the ruthenium atom with the lowest co-ordination number, *i.e.* a basal ruthenium with connectivity four rather than the apical ruthenium with a connectivity of five. The ability of $[Ru_5C(CO)_{15}]$ to act as an electron-pair acceptor will also be facilitated by the ease with which the metal framework may undergo rearrangement to produce vacant co-ordination sites (Figure 5). The final product $[Ru_5C(CO)_{15}(MeCN)]$ (2) has eight skeletal electron pairs and may therefore be regarded as an *arachno* pentagonal bipyramid. The ease with which the formation of these adducts may be reversed (see above) serves to emphasise the flexibility available to the Ru_5C framework as a result of the presence of the carbon atom which also acts to enhance the stability of the metal cluster; $[Ru_5C(CO)_{15}]$ (1) is stable to degradation by CO up to 400 atm at 100 °C for appreciable periods of time. It also demonstrates the importance of the donor properties of acetonitrile in reactions involving $[Ru_5C(CO)_{15}]$ (1).

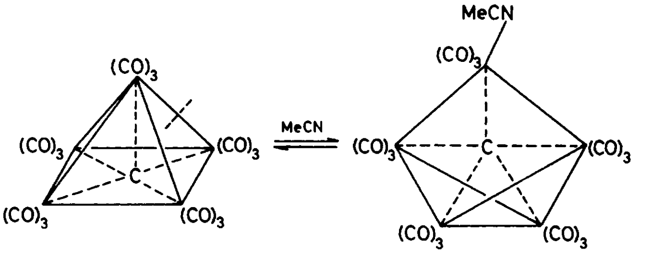

Figure 4. The reversible reaction of $[Ru_5C(CO)_{15}]$ with acetonitrile

A geometry similar to that of the Ru_5C skeleton in compound (2) has been observed previously in a number of phosphite-substituted Os_5 clusters,[10] and in the anion $[Os_5C(CO)_{15}I]^-$.[8] Exposed carbido-atoms bonded to tetranuclear Fe_4 butterfly clusters have also been observed.[11] Unlike the Ru_4 clusters $[Ru_4(CO)_{12}(C_2Ph_2)]$ [12] and $[Ru_4(CO)_{13}Cl]^-$ (ref. 13) the Ru(2)–Ru(3) hinge bond is *ca.* 0.16 Å shorter than the average value of 2.88(1) Å for the four hinge–wing-tip Ru–Ru bonds. The Ru(wing-tip)–Ru(5) bonds are of similar length [mean 2.88(1) Å] to the Ru(hinge)–Ru(wing-tip) bonds. The Ru–C (carbide) distances are of three types. The shortest are the Ru(wing-tip)–C(1) bonds [mean 1.97(2) Å], then the Ru(hinge)–C(1) bonds [mean 2.08(2) Å], and the longest is the Ru(5)–C(1) bond at 2.16(2) Å. Similar trends are observed in the structure of $[Os_5C(CO)_{15}I]^-$.[8] The average Ru–C(1) distance in compound (2) of 2.05(3) Å is similar to the average value of 2.06 Å in $[Ru_6C(CO)_{17}]$.[3] The Ru–C(carbonyl) distances for the butterfly metal atoms average 1.86(3) Å and all the carbonyls are effectively linear. For Ru(5) the two Ru–C(carbonyl) bonds *trans* to metal–metal bonds average 1.91(2) Å while the carbonyl *trans* to the linear MeCN group has a short Ru–C distance of 1.82(2) Å. This indicates strong Ru–CO back bonding for this C(53)O(53) ligand and a weak co-ordination of the MeCN ligand, in keeping with the long Ru(5)–N(1) bond distance.

The compound $[Ru_5C(CO)_{15}]$ (1) reacts rapidly with triphenylphosphine in dichloromethane to produce the monosubstituted compound $[Ru_5C(CO)_{14}(PPh_3)]$ (3a), which may

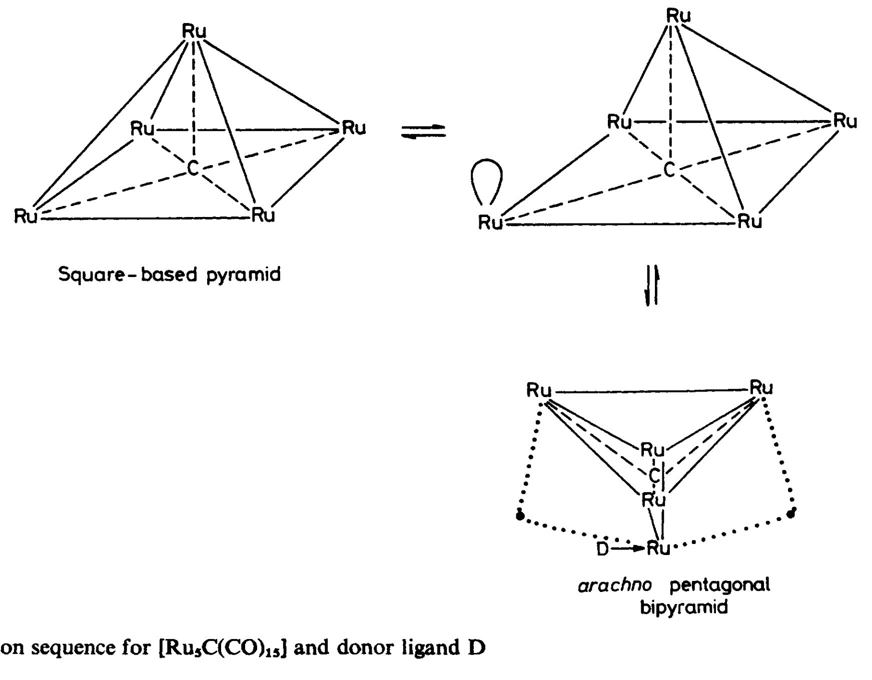

Figure 5. Possible reaction sequence for $[Ru_5C(CO)_{15}]$ and donor ligand D

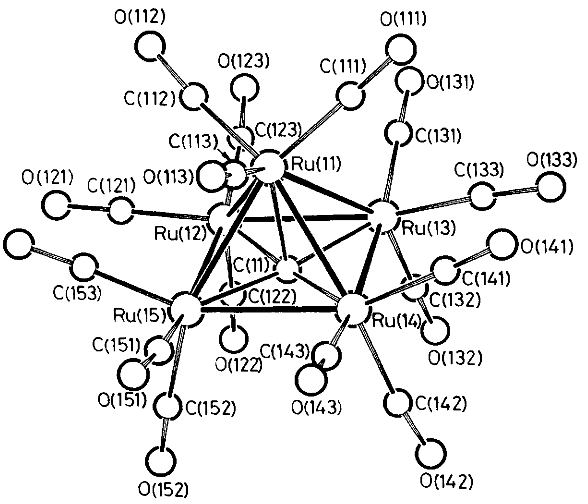

Figure 6. The molecular structure of $[Ru_5C(CO)_{15}]$ showing the atom-numbering scheme

also be obtained as the cluster product of the carbonylation of $[Ru_6C(CO)_{15}(PPh_3)_2]$ [equation (iv)]. On standing in the presence of excess of triphenylphosphine $[Ru_5C(CO)_{14}(PPh_3)]$ (3a) reacts further to produce the disubstituted compound $[Ru_5C(CO)_{13}(PPh_3)_2]$ (3b). The mechanism by which these substitution reactions occur has not been established. However, in view of the adduct formation with MeCN described above it is reasonable to suppose that these reactions proceed *via* an associative pathway although no direct evidence for the proposed intermediate $[Ru_5C(CO)_{15}(PPh_3)]$ has been found [equation (iv)]. This behaviour is a common feature of electron-deficient clusters and has been observed for a range of Os_5 and Os_6 cluster compounds.

$$\begin{tikzcd}
\underset{(1)}{[Ru_5C(CO)_{15}]} \arrow[r, "PPh_3"] & \text{‘}[Ru_5C(CO)_{15}(PPh_3)]\text{’} \arrow[r] & \underset{(3a)}{[Ru_5C(CO)_{14}(PPh_3)]} \\
{[Ru_6C(CO)_{17}]} \arrow[r, "PPh_3"] & {[Ru_6C(CO)_{15}(PPh_3)_2]} \arrow[ru, "CO", "700\text{ atm, }60\text{ °C, }0.5\text{ h}"'] &
\end{tikzcd}$$

(iv)

The structures of both $[Ru_5C(CO)_{14}(PPh_3)]$ (3a) and $[Ru_5C(CO)_{13}(PPh_3)_2]$ (3b) have been established by single-crystal *X*-ray analysis and are shown in Figure 2(*b*) and (*c*). Both retain the essentially square-pyramidal Ru_5C core found for the parent compound (1). In each molecule substitution has taken place at basal ruthenium atoms and the PPh_3 ligands occupy axial rather than equatorial sites. Attack of nucleophiles at basal atoms has been discussed above; the occupation of axial sites is presumably dictated by the steric demands of the bulky PPh_3 ligand. Steric interactions will also be minimised by the *trans* rather than the *cis* disposition of the phosphine ligands about the basal plane accounting for the ligand disposition observed for $[Ru_5C(CO)_{13}(PPh_3)_2]$.

The molecular structures of $[Ru_5C(CO)_{15}]$ (1), $[Ru_5C(CO)_{14}(PPh_3)]$ (3a), and $[Ru_5C(CO)_{13}(PPh_3)_2]$ (3b) are shown in Figures 6, 7, and 8 together with the atom-numbering schemes adopted. The asymmetric unit of structure (1) contains two independent but structurally similar molecules. Some comparative bond lengths and angles associated with these three structures are presented in Table 3. The structures of these complexes are closely related to the clusters $[M_5C(CO)_{15}]$ (M = Fe[7] or Os[8]). However, this series of ruthenium complexes gives a unique opportunity to study the structural changes upon substitution of carbonyl groups on basal metal atoms by one and two phosphine ligands. The Ru–Ru bond lengths in the square-based pyramidal metal skeletons show quite large variations which are difficult to interpret when individual bonds are considered in isolation. If the average values of each type of Ru–Ru bonds are considered some general statements can be made about trends in these three structures. The Ru(apical)–Ru(basal) bonds shorten slightly upon increasing substitution with average values of 2.83(2) Å for compound (1) and 2.81(2) Å for (3a) and (3b). The Ru(basal)–Ru(basal) bonds in (1) [average 2.86(2) Å] are longer than the Ru(apical)–Ru(basal) bonds. In the two substituted complexes the presence of the axial phosphine groups has little effect on the Ru(apical)–Ru(basal) bonds but in (3a) the two Ru(basal)–Ru(basal) bonds associated with the phosphine-substituted metal atom, Ru(3), are significantly longer [average 2.92(2) Å] compared to the average of 2.82(2) Å for the other two bonds. In compound (3b) where all four of the Ru(basal)–Ru(basal) bonds are associated with the phosphine-substituted metal atoms, Ru(2) and Ru(4), the average bond length of 2.88(2) Å is longer than for the unsubstituted cases. In both substituted complexes one Ru(basal)–Ru(basal) bond associated with the substituted metal atom is longer than the other.

The average Ru–C(carbide) distance also increases with increasing phosphine substitution, with values of 2.02(2), 2.04(2), and 2.05(2) Å, for complexes (1), (3a), and (3b), respectively. This increase in length is not mainly due to the lengthening of the Ru_4 basal framework but to the carbide atom moving further below the Ru_4 basal plane. In compound (1), C(1) lies 0.11(2) Å below the Ru_4 plane, while in (3a) the distance is 0.19(1) Å and in (3b) it is 0.23(1) Å.

The Ru–P bonds in complexes (3a) and (3b) are somewhat longer than the comparative values of 2.294(1) Å in $[Ru_3H(CO)_8(C{\equiv}CBu^t)\{PPh_2(OEt)\}]$[14] and 2.359(3) Å in $[Ru_6C(CO)_{16}(PEtPh_2)]$.[15] The distances are similar to the value of 2.380(6) Å in $[Ru_3(CO)_{11}(PPh_3)]$ where the phosphine occupies an equatorial site *trans* to an Ru–Ru bond.[16]

In the three complexes the partially exposed carbide is shielded from attack by the envelope of the ligands below the basal plane. In compound (1) the axial carbonyls on the four basal Ru atoms define a ‘ tunnel ’ of *ca.* 2 Å radius up which an incoming group would have to pass to attack the carbide directly. In (3a) a phenyl group of the axial phosphine lies under the Ru_4 square face and there is a contact distance of 2.42(2) Å between the carbide and H(12). In (3b) the phenyl rings on the two phosphine groups are orientated to close up the ‘ tunnel ’ some 3 Å below the basal Ru_4 plane, with the shortest contact distance of 2.76(2) Å between C(1) and H(212).

In all three clusters the carbonyl groups are all essentially linear and the average Ru–C(carbonyl) distances for (1), (3a), and (3b) are 1.88(2), 1.90(2), and 1.89(2) Å, respectively.

Similar reactions occur with the more basic phosphine $PMePh_2$, and with the bidentate phosphine $Ph_2P(CH_2)_nPPh_2$ (n = 1 or 2). With $PMePh_2$ the reaction occurs at a faster rate than with PPh_3 and a further substitution product, [Ru

Table 3. Selected bond lengths (Å) and angles (°) for $[Ru_5C(CO)_{15}]$ (1), $[Ru_5C(CO)_{14}(PPh_3)]$ (3a), and $[Ru_5C(CO)_{13}(PPh_3)_2]$ (3b)

	(1)			
	Molecule 1	Molecule 2	(3a)	(3b)
Ru(1)-Ru(2)	2.853(2)	2.811(2)	2.819(1)	2.787(2)
Ru(1)-Ru(3)	2.829(2)	2.872(2)	2.813(1)	2.804(2)
Ru(1)-Ru(4)	2.804(2)	2.800(2)	2.830(1)	2.832(2)
Ru(1)-Ru(5)	2.800(2)	2.838(2)	2.800(1)	2.815(2)
Ru(2)-Ru(3)	2.836(2)	2.838(2)	2.892(1)	2.919(2)
Ru(2)-Ru(5)	2.843(2)	2.847(2)	2.815(1)	2.889(2)
Ru(3)-Ru(4)	2.858(3)	2.859(2)	2.940(1)	2.845(2)
Ru(4)-Ru(5)	2.882(2)	2.876(2)	2.830(1)	2.864(2)
Ru(1)-C(1)	2.101(18)	2.078(17)	2.123(5)	2.163(8)
Ru(2)-C(1)	2.005(18)	2.030(17)	2.023(5)	2.070(8)
Ru(3)-C(1)	2.017(17)	2.029(17)	2.022(5)	2.044(7)
Ru(4)-C(1)	2.041(18)	2.019(17)	2.077(5)	2.076(8)
Ru(5)-C(1)	2.028(17)	2.004(18)	2.026(5)	2.004(7)
Ru(2)-P(1)	—	—	—	2.377(3)
Ru(3)-P(1)	—	—	2.377(1)	—
Ru(4)-P(2)	—	—	—	2.363(2)

	(1)			
	Molecule 1	Molecule 2	(3a)	(3b)
Ru(2)-C(1)-Ru(1)	88.0(7)	86.3(6)	85.6(2)	82.3(3)
Ru(3)-C(1)-Ru(1)	86.7(7)	88.7(7)	85.4(2)	83.5(3)
Ru(4)-C(1)-Ru(1)	85.2(7)	86.2(7)	84.7(2)	83.8(3)
Ru(5)-C(1)-Ru(1)	85.4(7)	88.1(7)	84.8(2)	84.9(3)
Ru(3)-C(1)-Ru(2)	89.7(7)	88.7(7)	91.3(2)	90.4(3)
Ru(4)-C(1)-Ru(2)	173.0(10)	172.0(10)	170.1(3)	166.1(5)
Ru(5)-C(1)-Ru(2)	89.6(7)	89.8(7)	93.2(2)	90.3(3)
Ru(4)-C(1)-Ru(3)	89.5(7)	89.9(7)	86.7(2)	87.4(3)
Ru(5)-C(1)-Ru(3)	172.0(1)	176.0(1)	169.1(3)	168.2(5)
Ru(5)-C(1)-Ru(4)	90.2(7)	91.2(7)	87.2(2)	89.2(3)

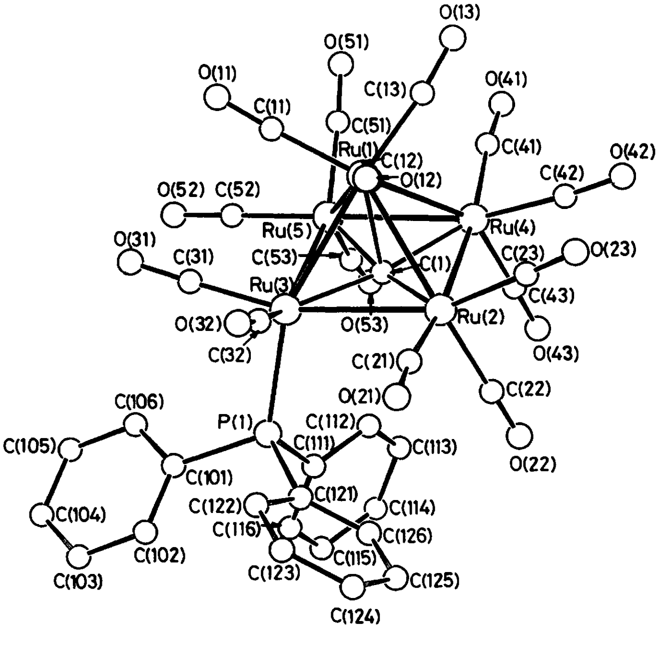

Figure 7. The molecular structure of $[Ru_5C(CO)_{14}(PPh_3)]$ showing the atom-numbering scheme

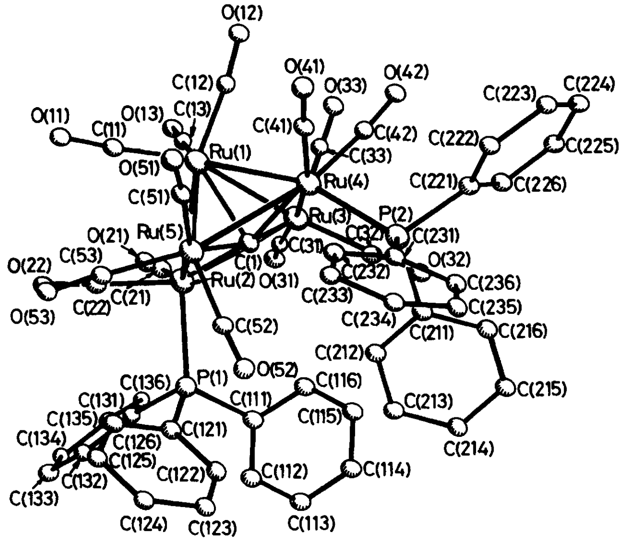

Figure 8. The molecular structure of $[Ru_5C(CO)_{13}(PPh_3)_2]$ showing the atom-numbering scheme

$(CO)_{12}(PMePh_2)_3]$ (4c), has been isolated. This derivative has been fully characterised on the basis of analytical, mass spectroscopic, and ^{31}P n.m.r. data but crystals suitable for *X*-ray analysis have not been obtained. As a consequence the site of attack of the third $PMePh_2$ ligand has not been determined.

The products of the reaction of $[Ru_5C(CO)_{15}]$ (1) with the diphosphines $Ph_2P(CH_2)_nPPh_2$ (n = 1 or 2) have been identified as $[Ru_5C(CO)_{13}\{Ph_2P(CH_2)_nPPh_2\}]$ [n = 1 (5) or 2 (6)] on the basis of their analytical and spectroscopic properties. In the ^{31}P n.m.r. spectrum of these molecules only one ^{31}P resonance is observed at −90 °C. This evidence combined with the observation that $[Ru_5(\mu\text{-}H)_2C(CO)_{12}\{Ph_2P(CH_2)_2PPh_2\}]$ (7) obtained from the hydrogenation of $[Ru_5C(CO)_{13}\{Ph_2P(CH_2)_2$-

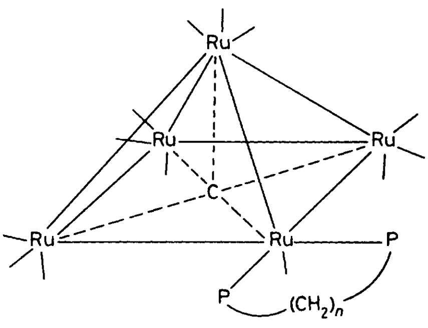

Figure 9. Proposed structure of $[Ru_5C(CO)_{13}\{Ph_2P(CH_2)_nPPh_2\}]$ (n = 1 or 2)

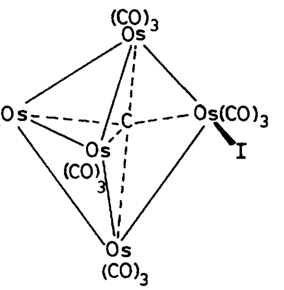

Figure 10. Representation of the structure of $[Os_5C(CO)_{15}I]^-$

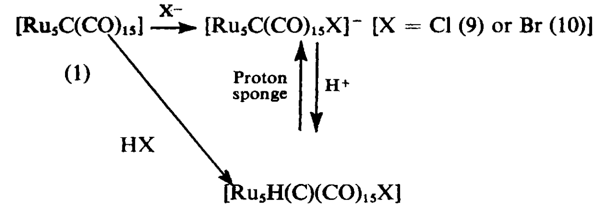

Scheme. Reaction of $[Ru_5C(CO)_{15}]$ with X^- or HX

$PPh_2\}]$ (see below) has the diphosphine ligand chelating one basal ruthenium atom leads us to propose the structure shown in Figure 9 for these compounds.

On treatment of $[Ru_5C(CO)_{15}]$ with halide ion, as in NEt_4X, a simple addition reaction occurs and the monoanions $[Ru_5C(CO)_{15}X]^-$ [X = F (8), Cl (9), Br (10), or I (11)] are produced. These anions have i.r. spectra in the ν(CO) region which are very similar to that observed for $[Os_5C(CO)_{15}I]^-$ (ref. 8) and for which an *arachno* pentagonal-bipyramidal metal arrangement closely related to that of $[Ru_5C(CO)_{15}(MeCN)]$ (2) has been established (Figure 10).

Protonation of these anions with concentrated H_2SO_4 yields the monohydrido-compounds $[Ru_5H(C)(CO)_{15}X]$, which may also be prepared by the direct reaction of HX (X = Cl or Br) with $[Ru_5C(CO)_{15}]$ (1). The ^1H n.m.r. spectra of these species show one high-field resonance due to the bonded hydrido-ligand and clearly indicate that H^+ addition has not occurred on the carbido-atom. On reaction of the hydrido-species with proton sponge [1,8-bis(dimethylamino)naphthalene] in dichloromethane the anions $[Ru_5C(CO)_{15}X]^-$ are regenerated. These reactions are summarised in the Scheme.

The reactions that $[Ru_5C(CO)_{15}]$ (1) undergoes with halogens X_2 [X = Cl (12), Br (13), or I (14)] depend upon the nature of X. With Cl_2 or Br_2 the cluster appears to undergo complete fragmentation to produce the dimer $[Ru_2(CO)_6X_4]$.

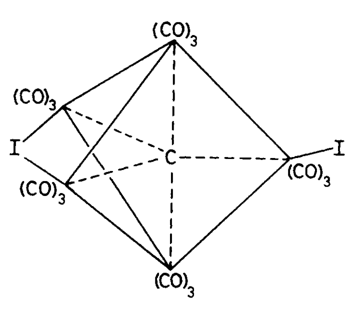

Figure 11. Probable structure of $[Ru_5C(CO)_{15}I_2]$

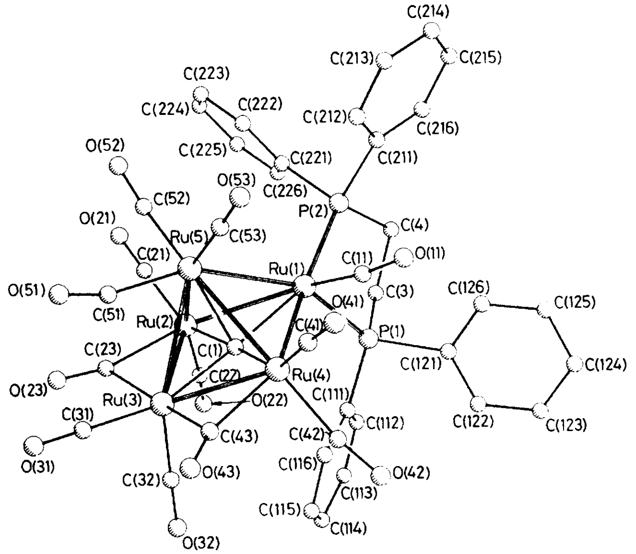

Figure 12. The molecular structure of $[Ru_5(\mu\text{-}H)_2C(CO)_{12}\{Ph_2P(CH_2)_2PPh_2\}]$ including the atom-numbering scheme

Yields of these dimers are almost quantitative and it is tempting to speculate that the carbido-atom is lost as CX_4; however, no evidence for this compound has been found. In contrast, reaction with I_2 leads to the simple addition compound $[Ru_5C(CO)_{15}I_2]$. Infrared studies on this molecule indicate that the five metal atoms designate a bridged butterfly arrangement and we should expect that the structure would be as shown in Figure 11.

The various tertiary phosphine-substituted derivatives (see above) all react with hydrogen. In general several products are obtained and these have not been fully characterised to date. An exception is the product of the reaction of $[Ru_5C(CO)_{13}\{Ph_2P(CH_2)_2PPh_2\}]$ (6) with H_2 which has been identified by spectroscopic and single-crystal *X*-ray analysis as $[Ru_5(\mu\text{-}H)_2C(CO)_{12}\{Ph_2P(CH_2)_2PPh_2\}]$ (7). The asymmetric unit contains two independent but structurally similar molecules one of which is shown in Figure 12. Selected bond lengths and angles are presented in Table 4. The overall geometry of the Ru_5C core is similar to that of the complexes (1), (3a), and (3b). However, the distribution of the carbonyl groups is different. Three of the Ru atoms in the basal plane each have two terminal carbonyl groups bonded to them, and the Ru(2)–Ru(3) [molecule 2, Ru(7)–Ru(8)] and the Ru(3)–Ru(4)[Ru(8)–Ru(9)] edges are asymmetrically bridged by carbonyl ligands. The fourth basal metal atom, Ru(1) [Ru(6)], has one equatorial carbonyl ligand co-ordinated to it and the chelating $Ph_2P(CH_2)_2PPh_2$ ligand of which one P atom occupies an axial site and the other an equatorial site. The

Table 4. Selected bond lengths (Å) and angles (°) for $[Ru_5(\mu\text{-}H)_2C(CO)_{12}\{Ph_2P(CH_2)_2PPh_2\}]$ (7)

	Molecule 1	Molecule 2		Molecule 1	Molecule 2
Ru(1)-Ru(2)	2.932(4)	2.949(4)	Ru(1)-C(1)-Ru(2)	96.0(13)	93.5(12)
Ru(1)-Ru(4)	2.928(4)	2.935(5)	Ru(1)-C(1)-Ru(3)	172.3(15)	169.9(12)
Ru(1)-Ru(5)	2.864(4)	2.885(5)	Ru(2)-C(1)-Ru(3)	88.2(10)	85.7(9)
Ru(2)-Ru(3)	2.752(5)	2.797(5)	Ru(1)-C(1)-Ru(4)	90.6(10)	93.8(9)
Ru(2)-Ru(5)	2.837(4)	2.827(4)	Ru(2)-C(1)-Ru(4)	169.1(16)	163.5(14)
Ru(3)-Ru(4)	2.773(4)	2.745(5)	Ru(3)-C(1)-Ru(4)	84.4(11)	84.5(11)
Ru(3)-Ru(5)	2.911(4)	2.898(4)	Ru(1)-C(1)-Ru(5)	86.1(9)	85.5(9)
Ru(4)-Ru(5)	2.861(5)	2.835(5)	Ru(2)-C(1)-Ru(5)	87.5(10)	82.5(9)
Ru(1)-C(1)	2.022(27)	2.005(26)	Ru(3)-C(1)-Ru(5)	87.6(11)	84.4(9)
Ru(2)-C(1)	1.923(27)	2.043(25)	Ru(4)-C(1)-Ru(5)	84.2(9)	83.4(8)
Ru(3)-C(1)	2.031(28)	2.070(27)	Ru(1)-P(1)-C(3)	106.2(10)	107.4(10)
Ru(4)-C(1)	2.096(28)	2.014(25)	Ru(1)-P(2)-C(4)	110.0(9)	108.4(11)
Ru(5)-C(1)	2.171(26)	2.239(23)			
Ru(1)-P(1)	2.318(8)	2.341(8)			
Ru(1)-P(2)	2.348(9)	2.342(9)			

apical metal atom, Ru(5)[Ru(10)], is bonded to three terminal carbonyl ligands. The two hydride ligands were not located in the analysis. However, potential-energy calculations using the method developed by Orpen[17] for locating hydrides indicates that they bridge the Ru(1)–Ru(2)[Ru(6)–Ru(7)] bond in the basal plane and the basal–apical Ru(1)–Ru(5)[Ru(6)–Ru(10)] bond. With this arrangement of ligands each metal atom does not obey the 18-electron rule; Ru(1) [Ru(6)] has 19 electrons and Ru(4)[Ru(9)] only 17. The imbalance is partially overcome by the incipient bridge bond from the carbonyl C(11)O(11)[C(61)O(61)] on Ru(1)[Ru(6)] to Ru(4)[Ru(9)] indicated by the short C(11) ··· Ru(4) contact distance of 2.774(40) Å [C(61) ··· Ru(9) 2.722(40) Å] and the bending of the carbonyl group Ru(1)–C(11)–O(11) 169.1(30)° [Ru(6)–C(61)–O(61) 169.4(32)°].

The ^{31}P n.m.r. spectrum of the orange product consists of two singlets [−79.2 and −86.6 p.p.m., $P(OMe)_3$ standard] showing the two phosphorus atoms in the diphosphine ligand to be inequivalent in solution at 24 °C. The ^{1}H n.m.r. spectrum in the high-field region, recorded at the same temperature, consists of two doublets of doublets. For the first proton (δ *ca.* −13) the two coupling constants $J(H^1\text{–}P^1)$ and $J(H^1\text{–}P^2)$ are very similar (13.78 and 17.73 Hz), while for the second proton (δ *ca.* −19), $J(H^2\text{–}P^1)$ and $J(H^2\text{–}P^2)$ are very different (25.60 and 7.88 Hz), indicating the presence of two metal hydrides in different environments.

These data are consistent with the prediction of hydride positions from crystallographic measurements, since a hydride ligand bridging Ru(1)–Ru(2) would be expected to couple moderately strongly, and more or less equally, to P(1) and P(2), whereas a hydride ligand bridging Ru(1)–Ru(5) would be expected to couple strongly to P(1) and weakly to P(2).

The variation in the Ru–Ru bond lengths in (7) is somewhat greater than in the complexes (1), (3a), and (3b) because of the presence of different edge-bridging ligands. The average carbonyl-bridged basal Ru–Ru bond length is 2.77(2) Å which is *ca.* 0.06 Å shorter than the value in $[Ru_5C(CO)_{15}]$ (1), whilst the average hydride-bridged basal Ru–Ru bond is considerably longer at 2.94(1) Å. These distances are in keeping with the normal bond-shortening and bond-lengthening effects of a bridging carbonyl and hydride, respectively. The average unbridged basal Ru–Ru bond length of 2.93(1) Å, which is *trans* to a Ru–P bond, is also significantly longer than the basal Ru–Ru bonds in compound (1). The average basal–apical hydride-bridged Ru–Ru bond length in (7) is 2.88(1) Å which is only *ca.* 0.02 Å longer than the average for the unbridged basal–axial bonds. Both the bridged and unbridged axial–basal bonds in (7) are longer than the equivalent bonds in $[Ru_5C(CO)_{15}]$ (1).

The average Ru(basal)–C(carbide) of 2.03(2) Å is similar to that in the other square-pyramidal ruthenium cluster complexes. The carbide lies 0.17 Å below the basal plane, a distance similar to that in the phosphine disubstituted complex (3b).

The average Ru–P(axial) bond length of 2.33(2) Å is marginally shorter than the value of 2.35(1) Å for the Ru–P(equatorial) bonds. In the complex $[Ru_4H_4(CO)_{10}\{Ph_2P(CH_2)_2PPh_2\}]$,[18] where the diphosphine ligand also chelates one Ru atom, the two Ru–P distances of 2.303(2) and 2.321(2) Å are slightly shorter than in (7). However, in a second isomer of $[Ru_4H_4(CO)_{10}\{Ph_2P(CH_2)_2PPh_2\}]$,[19] where the diphosphine bridges two metal atoms, the slightly longer Ru–P distances of 2.356(4) and 2.335(5) Å are more in keeping with the values in (7).

On treatment of $[Ru_5H_2C(CO)_{12}\{Ph_2P(CH_2)_2PPh_2\}]$ with H_2 a further hydrogenation product is obtained. This product, which seems from its ^{1}H n.m.r. spectrum to contain more hydride ligands and which may have a more open structure, is currently the subject of further investigation.

It is perhaps surprising that on pyrolysis under argon $[Ru_5C(CO)_{15}]$ is converted back into $[Ru_6C(CO)_{17}]$ in about 60% yield. This reaction is accompanied by the production of some ruthenium metal and a species which is clearly anionic.

Experimental

The cluster $[Ru_6C(CO)_{17}]$ was prepared by the literature method. Infrared spectra were recorded as solutions in 0.5-mm CaF_2 cells on a Perkin-Elmer 257 spectrometer with carbon monoxide as calibrant. Mass spectra were obtained using an A.E.I. M.S. 12 instrument at 70 eV ionising potential. Hydrogen-1 n.m.r. spectra were recorded on a Brucker WH 400 spectrometer (400 MHz) using CD_2Cl_2 as solvent and $SiMe_4$ as reference, ^{31}P spectra on a Brucker WH 250 spectrometer (250 MHz) using CD_2Cl_2 as solvent and $P(OMe)_3$ as reference. Thin-layer chromatography plates (Merck) consisted of 20 × 20 cm glass plates coated with a 0.3-mm layer of silica gel. Reactions with carbon monoxide or hydrogen were carried out in Roth (120 cm^3) magnetically stirred autoclaves using heptane as solvent.

Preparation of $[Ru_5C(CO)_{15}]$.—The compound $[Ru_6C(CO)_{17}]$ (250 mg) was placed in an autoclave with heptane (50 cm^3). The autoclave was pressurised twice to 30 atm carbon mon-

Table 5. Molecular structure determination data

	(1)	(2)	(3a)	(3b)	(7)
Molecular formula	$C_{16}O_{15}Ru_5$	$C_{18}H_3NO_{15}Ru_5$	$C_{33}H_{15}O_{14}PRu_5$	$C_{51}H_{30}O_{13}P_2Ru_5$	$C_{39}H_{26}O_{12}P_2Ru_5$
Molecular weight	937.51	978.56	1 171.77	1 406.03	1 283.91
Colour	Red	Red-orange	Red	Red	Red
Crystal habit	Plate	Block	Block	Block	Plate
Crystal dimensions (mm)	0.16 × 0.108 × 0.02	0.35 × 0.28 × 0.25	0.15 × 0.12 × 0.11	0.23 × 0.16 × 0.12	0.23 × 0.19 × 0.04
Space group	$P2_1/c$	$P2_1/n$	Pn	$P2_1/c$	$P2_1$
a/Å	16.448(3)	14.116(6)	9.953(2)	15.923(4)	12.210(4)
b/Å	14.274(2)	18.167(7)	12.247(2)	12.494(3)	18.602(6)
c/Å	20.834(4)	10.276(4)	14.703(3)	25.210(7)	18.409(6)
β/°	91.36(2)	95.14(3)	91.23(2)	93.28(2)	97.63(2)
U/Å^3	4 890.0	2 624.6	1 791.8	5 007.1	4 144.3
D_c/g cm^{-3}	2.55	2.48	2.17	1.86	2.06
Z	8	4	2	4	4
F(000)	3 488	1 832	1 220	2 736	2 424
μ(Mo-K_α)	28.10	28.01	21.81	15.39	18.50
Diffractometer	Phillips PW1100	Syntex $P2_1$	Stoe	Stoe	Stoe
2θ range (°) min.	3.0	3.0	7.0	3.0	3.0
max.	50.0	45.0	50.0	50.0	50.0
No. reflections measured	3 984	2 541	3 508	5 186	5 810
Scan mode	ω—2θ	ω—2θ	ω—θ	ω—θ	ω—θ
No. steps in scan	30	96	24	140	120
Step width (°)	0.05	Variable	Variable	0.01	0.01
Minimum counts for reflection to be measured (counts s^{-1})	10	7	0	8	4
$F > n\sigma(F)$ n =	6	4	3	3	3
No. unique observed reflections	3 256	1 604	3 305	4 127	3 510
Method of absorption correction	None	Empirical 422 Azimuthal scan data	Empirical 372 Azimuthal scan data	Empirical 464 Azimuthal scan data	Empirical 368 Azimuthal scan data
Transmission factors					
min.	—	0.902	0.531	0.874	0.822
max.	—	0.988	0.576	0.922	1.000
Method of Ru atom location	Patterson	Σ_2 sign expansion	Tangent expansion	Σ_2 sign expansion	Tangent expansion
Refinement technique (least squares)	Blocked full matrix	Blocked cascade	Blocked cascade	Blocked cascade	Blocked cascade
Weighting scheme w	$[\sigma^2(F)]^{-1}$	$[\sigma^2(F)]^{-1}$	$[\sigma^2(F) + 0.000\,27\lvert F\rvert^2]^{-1}$	$[\sigma^2(F)]^{-1}$	$[\sigma^2(F) + 0.0002\lvert F\rvert]^{-1}$
Converged residuals					
R	0.051	0.047	0.021	0.039	0.064
$R' = \Sigma w^{\frac{1}{2}}\Delta/\Sigma w^{\frac{1}{2}}\lvert F_o\rvert$	0.050	0.039	0.022	0.036	0.054
Cell determined from n reflections in	25	15	42	20	20
2θ range (°)	15 < 2θ < 25	15 < 2θ < 25	20 < 2θ < 30	15 < 2θ < 25	15 < 2θ < 25

Details pertaining to all structures: crystal system, monoclinic; D_m, not measured; Mo-$K\alpha$ radiation, λ = 0.710 69 Å; step time, 0.5 s; method of light atom location, Fourier difference.

Table 6. Fractional atomic co-ordinates for [$Ru_5C(CO)_{15}$]

Atom	*x*	*y*	*z*	Atom	*x*	*y*	*z*
Ru(11)	0.324 17(11)	0.360 50(12)	0.265 74(8)	C(152)	0.454 2(15)	0.103 7(19)	0.185 4(12)
Ru(12)	0.325 65(11)	0.175 10(12)	0.316 85(8)	O(152)	0.463 2(10)	0.027 3(13)	0.169 1(8)
Ru(13)	0.188 53(10)	0.241 41(13)	0.245 30(9)	C(153)	0.514 1(13)	0.239 5(16)	0.277 6(11)
Ru(14)	0.290 74(11)	0.291 93(13)	0.141 80(8)	O(153)	0.570 6(11)	0.250 6(14)	0.311 6(9)
Ru(15)	0.429 78(10)	0.226 61(13)	0.215 76(1)	C(1)	0.307 8(10)	0.225 3(12)	0.227 7(9)
Ru(21)	0.267 57(10)	0.708 54(12)	0.015 33(8)	C(211)	0.292 6(15)	0.598 6(19)	−0.029 9(13)
Ru(22)	0.255 41(10)	0.889 87(12)	−0.036 64(8)	O(211)	0.306 3(11)	0.528 1(14)	−0.054 3(9)
Ru(23)	0.177 05(10)	0.739 56(12)	−0.102 31(8)	C(212)	0.372 6(15)	0.752 8(18)	0.016 4(12)
Ru(24)	0.098 41(10)	0.686 11(12)	0.013 00(8)	O(212)	0.440 8(11)	0.775 4(13)	0.018 5(9)
Ru(25)	0.171 11(11)	0.844 82(12)	0.077 08(8)	C(213)	0.271 0(15)	0.659 1(18)	0.097 0(13)
C(111)	0.239 0(13)	0.446 6(16)	0.271 7(10)	O(213)	0.274 8(11)	0.622 0(13)	0.148 2(9)
O(111)	0.188 0(11)	0.504 0(12)	0.274 0(8)	C(221)	0.331 9(13)	0.959 7(16)	0.009 4(11)
C(112)	0.364 4(14)	0.370 4(17)	0.350 9(12)	O(221)	0.384 2(10)	1.006 1(11)	0.034 2(8)
O(112)	0.387 4(11)	0.387 5(13)	0.403 6(9)	C(222)	0.195 7(14)	0.992 1(17)	−0.061 4(11)
C(113)	0.395 5(14)	0.444 4(17)	0.226 8(11)	O(222)	0.156 3(10)	1.055 3(13)	−0.077 3(8)
O(113)	0.438 6(11)	0.500 6(12)	0.203 0(9)	C(223)	0.327 3(13)	0.893 6(16)	−0.105 9(11)
C(121)	0.417 0(14)	0.149 5(16)	0.367 2(11)	O(223)	0.367 9(10)	0.899 0(12)	−0.149 4(8)
O(121)	0.473 7(10)	0.130 1(12)	0.400 1(8)	C(231)	0.248 0(13)	0.744 3(16)	−0.169 6(11)
C(122)	0.309 2(15)	0.045 5(20)	0.302 0(13)	O(231)	0.290 5(10)	0.744 0(12)	−0.215 4(9)
O(122)	0.303 7(10)	−0.032 3(13)	0.293 0(9)	C(232)	0.097 5(12)	0.807 4(15)	−0.143 9(10)
C(123)	0.264 9(15)	0.180 4(18)	0.392 5(12)	O(232)	0.045 8(10)	0.854 8(12)	−0.170 8(8)
O(123)	0.233 6(11)	0.184 5(13)	0.442 1(10)	C(233)	0.142 3(13)	0.627 4(17)	−0.138 2(11)
C(131)	0.126 0(15)	0.249 1(19)	0.320 4(13)	O(233)	0.118 6(9)	0.556 7(12)	−0.161 3(8)
O(131)	0.087 5(11)	0.259 4(14)	0.365 4(9)	C(241)	0.090 9(13)	0.559 7(17)	−0.017 4(11)
C(132)	0.147 5(13)	0.123 0(17)	0.221 6(11)	O(241)	0.087 2(10)	0.483 6(12)	−0.033 4(8)
O(132)	0.121 1(10)	0.051 4(13)	0.205 8(8)	C(242)	−0.009 5(14)	0.725 0(16)	−0.009 3(11)
C(133)	0.106 4(16)	0.312 4(19)	0.204 5(14)	O(242)	−0.072 2(11)	0.749 4(13)	−0.024 4(9)
O(133)	0.048 4(12)	0.349 5(14)	0.177 4(10)	C(243)	0.069 5(13)	0.637 9(16)	0.095 2(12)
C(141)	0.216 2(15)	0.381 0(18)	0.112 6(12)	O(243)	0.052 9(9)	0.604 4(11)	0.141 3(8)
O(141)	0.173 1(11)	0.442 4(14)	0.093 6(9)	C(251)	0.136 8(14)	0.798 0(17)	0.154 5(12)
C(142)	0.259 6(16)	0.198 2(20)	0.084 1(13)	O(251)	0.112 2(11)	0.780 8(13)	0.207 2(10)
O(142)	0.231 1(12)	0.139 0(15)	0.053 2(10)	C(252)	0.091 6(15)	0.938 1(18)	0.074 7(12)
C(143)	0.360 4(19)	0.340 4(22)	0.084 5(16)	O(252)	0.041 0(11)	0.996 6(13)	0.065 8(9)
O(143)	0.403 3(15)	0.383 7(18)	0.048 0(13)	C(253)	0.246 9(17)	0.916 3(20)	0.121 5(14)
C(151)	0.498 0(14)	0.287 1(17)	0.157 3(12)	O(253)	0.295 2(12)	0.955 2(15)	0.152 3(10)
O(151)	0.545 7(11)	0.321 7(13)	0.126 5(9)	C(2)	0.170 5(10)	0.793 7(12)	−0.012 5(8)

Table 7. Atom co-ordinates (× 10^4) for [$Ru_5C(CO)_{15}(MeCN)$]

Atom	*x*	*y*	*z*	Atom	*x*	*y*	*z*
Ru(1)	8 503(1)	854(1)	3 057(1)	O(31)	6 252(10)	−552(7)	305(14)
Ru(2)	6 976(1)	1 604(1)	4 198(2)	C(32)	5 267(15)	248(11)	3 129(20)
Ru(3)	6 550(1)	360(1)	2 794(2)	O(32)	4 479(10)	134(8)	3 332(15)
Ru(4)	6 126(1)	1 766(1)	1 567(2)	C(33)	6 916(15)	−360(12)	4 011(10)
Ru(5)	8 033(1)	1 734(1)	767(2)	O(33)	7 099(10)	−827(8)	4 821(14)
C(1)	7 922(13)	1 294(9)	2 341(17)	C(41)	6 097(15)	2 824(12)	1 488(20)
C(11)	9 107(14)	171(10)	2 016(19)	O(41)	5 993(13)	3 446(8)	1 461(15)
O(11)	9 454(12)	−246(9)	1 362(14)	C(42)	4 920(16)	1 737(12)	2 132(21)
C(12)	9 554(16)	1 451(12)	3 449(20)	O(42)	4 106(12)	1 744(10)	2 387(18)
O(12)	10 204(10)	1 844(9)	3 631(15)	C(43)	5 729(15)	1 490(11)	−152(20)
C(13)	8 780(14)	308(11)	4 599(20)	O(43)	5 503(10)	1 332(8)	−1 250(13)
O(13)	8 981(11)	−60(8)	5 528(14)	C(51)	7 558(14)	2 301(11)	−727(20)
C(21)	7 641(16)	1 338(12)	5 798(22)	O(51)	7 274(10)	2 665(8)	−1 599(13)
O(21)	8 080(17)	1 256(11)	6 810(16)	C(52)	9 306(14)	1 668(11)	307(18)
C(22)	7 243(17)	2 576(13)	4 464(23)	O(52)	10 101(11)	1 649(8)	92(17)
O(22)	7 326(13)	3 230(9)	4 621(16)	C(53)	9 310(15)	2 553(11)	1 753(19)
C(23)	5 889(17)	1 592(13)	4 885(22)	O(53)	8 547(9)	3 072(7)	2 400(12)
O(23)	5 102(15)	1 593(9)	5 355(19)	N(1)	7 789(11)	764(8)	−357(14)
C(31)	6 418(14)	−215(11)	1 256(20)	C(2)	7 777(14)	271(10)	−981(19)
				C(3)	7 803(14)	−372(10)	−1 819(18)

oxide, then vented to atmospheric pressure, pressurised to 80 atm carbon monoxide, and heated to 80 °C for 3 h. It was then cooled, the pressure released, and the red solution evaporated to dryness. The red solid was extracted into hexane and filtered. Slow evaporation of the hexane solution produced red crystals of [$Ru_5C(CO)_{15}$] (1) (208 mg, 97.2%).

Reactions of [$Ru_5C(CO)_{15}$].—(*a*) *With* PPh_3. Addition of 1 equivalent of PPh_3 to [$Ru_5C(CO)_{15}$] (1) in CH_2Cl_2 gave a pink solution of [$Ru_5C(CO)_{14}(PPh_3)$] (3a). Addition of an excess of PPh_3 to a solution of (1) in CH_2Cl_2 gave a mixture of (3a) and [$Ru_5C(CO)_{13}(PPh_3)_2$] (3b), which may be separated by t.l.c. in 10% diethyl ether–hexane. On standing for several

Table 8. Atomic co-ordinates ($\times 10^4$) for $[Ru_5C(CO)_{14}(PPh_3)]$

Atom	*x*	*y*	*z*	Atom	*x*	*y*	*z*
Ru(1)	1 231	430(1)	9 672	O(43)	−2 074(5)	1 747(4)	6 687(3)
Ru(2)	−828(1)	2 010(1)	9 610(1)	C(51)	2 532(6)	−450(4)	7 668(4)
Ru(3)	1 959(1)	2 628(1)	9 432(1)	O(51)	2 822(6)	−1 336(4)	7 525(4)
Ru(4)	−627(1)	482(1)	8 189(1)	C(52)	3 934(6)	1 424(5)	7 895(4)
Ru(5)	2 103(1)	1 031(1)	7 945(1)	O(52)	5 061(5)	1 648(5)	7 790(4)
C(1)	651(5)	1 666(4)	8 731(3)	C(53)	1 743(6)	1 504(4)	6 725(4)
C(11)	3 092(6)	116(5)	9 880(4)	O(53)	1 493(6)	1 753(4)	5 997(3)
O(11)	4 191(5)	−87(5)	10 037(4)	P(1)	1 746(1)	4 482(1)	8 971(1)
C(12)	768(8)	548(6)	10 911(5)	C(101)	3 266(5)	5 323(4)	8 924(3)
O(12)	596(8)	571(5)	11 683(3)	C(102)	3 317(6)	6 414(4)	9 247(4)
C(13)	654(7)	−1 039(5)	9 501(5)	C(103)	4 451(6)	7 041(4)	9 094(4)
O(13)	410(7)	−1 949(4)	9 465(5)	C(104)	5 500(6)	6 641(5)	8 605(4)
C(21)	−791(6)	2 928(4)	10 669(4)	C(105)	5 459(6)	5 600(5)	8 283(5)
O(21)	−878(5)	3 449(4)	11 305(3)	C(106)	4 330(6)	4 922(5)	8 445(4)
C(22)	−1 970(6)	2 946(4)	8 919(4)	C(111)	1 031(5)	4 741(4)	7 829(3)
O(22)	−2 680(5)	3 452(4)	8 459(3)	C(112)	372(6)	3 946(4)	7 351(3)
C(23)	−2 242(6)	1 197(5)	10 157(4)	C(113)	−102(7)	4 129(5)	6 470(4)
O(23)	−3 050(5)	715(4)	10 514(3)	C(114)	80(6)	5 120(5)	6 073(4)
C(31)	3 838(6)	2 635(4)	9 516(3)	C(115)	742(8)	5 936(5)	6 542(4)
O(31)	4 985(4)	2 612(4)	9 649(3)	C(116)	1 214(7)	5 752(5)	7 424(4)
C(32)	2 039(5)	2 956(4)	10 686(4)	C(121)	651(5)	5 227(4)	9 737(3)
O(32)	2 159(5)	3 090(4)	11 447(3)	C(122)	−669(6)	5 473(4)	9 489(4)
C(41)	−322(6)	−748(5)	7 411(4)	C(123)	−1 487(7)	5 963(5)	10 127(4)
O(41)	−230(7)	−1 472(5)	6 936(5)	C(124)	−1 021(7)	6 223(5)	10 971(4)
C(42)	−2 236(7)	−213(6)	8 596(4)	C(125)	288(7)	6 014(5)	11 216(4)
O(42)	−3 165(6)	−677(5)	8 822(5)	C(126)	1 121(6)	5 496(4)	10 600(3)
C(43)	−1 524(7)	1 265(5)	7 240(4)				

Table 9. Atom co-ordinates ($\times 10^4$) for $[Ru_5C(CO)_{13}(PPh_3)_2]$

Atom	*x*	*y*	*z*	Atom	*x*	*y*	*z*
Ru(1)	7 167(1)	−173(1)	4 392(1)	C(112)	7 172(4)	721(5)	1 428(3)
Ru(2)	7 343(1)	−419(1)	3 305(1)	C(113)	6 682(4)	1 390(5)	1 093(3)
Ru(3)	6 130(1)	1 087(1)	3 707(1)	C(114)	6 088(4)	2 066(5)	1 303(3)
Ru(4)	7 408(1)	2 072(1)	4 375(1)	C(115)	5 984(4)	2 074(5)	1 849(3)
Ru(5)	8 626(1)	655(1)	3 964(1)	C(116)	6 474(4)	1 406(5)	2 184(3)
C(1)	7 411(5)	952(6)	3 767(3)	C(121)	8 778(3)	256(4)	2 345(3)
C(11)	7 965(6)	−1 231(8)	4 617(5)	C(122)	8 965(3)	1 232(4)	2 111(3)
O(11)	8 402(5)	−1 920(6)	4 764(4)	C(123)	9 800(3)	1 555(4)	2 085(3)
C(12)	6 984(6)	322(8)	5 088(5)	C(124)	10 448(3)	900(4)	2 293(3)
O(12)	6 682(6)	510(6)	5 515(4)	C(125)	10 261(3)	−76(4)	2 527(3)
C(13)	6 202(6)	−1 098(7)	4 334(4)	C(126)	9 426(3)	−399(4)	2 553(3)
O(13)	5 655(4)	−1 671(6)	4 307(4)	C(131)	7 579(3)	−1 389(5)	1 998(3)
P(1)	7 688(1)	−168(2)	2 409(1)	C(132)	8 259(3)	−1 906(5)	1 785(3)
C(21)	6 486(6)	−1 412(8)	3 134(4)	C(133)	8 122(3)	−2 786(5)	1 451(3)
O(21)	6 021(4)	−2 093(6)	3 049(4)	C(134)	7 306(3)	−3 150(5)	1 330(3)
C(22)	8 044(6)	−1 621(7)	3 361(4)	C(135)	6 625(3)	−2 633(5)	1 543(3)
O(22)	8 414(4)	−2 404(5)	3 393(3)	C(136)	6 762(3)	−1 753(5)	1 877(3)
C(31)	5 404(7)	301(9)	3 233(5)	C(211)	7 468(4)	4 152(4)	3 381(3)
O(31)	4 913(5)	−94(7)	2 947(4)	C(212)	7 641(4)	3 395(4)	2 995(3)
C(32)	5 789(6)	2 380(8)	3 370(4)	C(213)	7 545(4)	3 662(4)	2 458(3)
O(32)	5 551(4)	3 159(5)	3 176(3)	C(214)	7 276(4)	4 685(4)	2 306(3)
C(33)	5 266(6)	1 079(8)	4 203(4)	C(215)	7 103(4)	5 442(4)	2 692(3)
O(33)	4 732(4)	1 034(7)	4 485(3)	C(216)	7 199(4)	5 175(4)	3 229(3)
P(2)	7 698(1)	3 822(2)	4 081(1)	C(221)	7 092(3)	4 795(5)	4 450(3)
C(41)	8 040(6)	2 380(7)	5 014(5)	C(222)	7 466(3)	5 291(5)	4 899(3)
O(41)	8 369(5)	2 558(6)	5 423(3)	C(223)	6 995(3)	5 978(5)	5 202(3)
C(42)	6 448(6)	2 574(8)	4 683(4)	C(224)	6 150(3)	6 168(5)	5 055(3)
O(42)	5 874(4)	2 846(6)	4 903(3)	C(225)	5 777(3)	5 671(5)	4 606(3)
C(51)	9 245(6)	951(7)	4 617(4)	C(226)	6 248(3)	4 985(5)	4 303(3)
O(51)	9 646(5)	1 089(6)	4 999(4)	C(231)	8 775(4)	4 345(4)	4 193(3)
C(52)	9 233(6)	1 610(7)	3 532(4)	C(232)	9 443(4)	3 672(4)	4 349(3)
O(52)	9 599(4)	2 192(5)	3 308(3)	C(233)	10 261(4)	4 075(4)	4 396(3)
C(53)	9 391(6)	−482(8)	3 855(4)	C(234)	10 411(4)	5 150(4)	4 288(3)
O(53)	9 903(4)	−1 125(5)	3 802(3)	C(235)	9 743(4)	5 824(4)	4 132(3)
C(111)	7 068(4)	729(5)	1 974(3)	C(236)	8 925(4)	5 421(4)	4 085(3)

Table 10. Atom co-ordinates (× 10^4) for $[Ru_5(\mu\text{-}H)_2C(CO)_{12}\{Ph_2P(CH_2)_2PPh_2\}]$

Atom	*x*	*y*	*z*	Atom	*x*	*y*	*z*
Ru(1)	5 944(2)	3 359	2 586(1)	Ru(6)	10 942(2)	8 729(1)	2 906(1)
Ru(2)	5 179(2)	3 462(2)	1 011(1)	Ru(7)	10 120(2)	8 462(2)	1 349(1)
Ru(3)	4 867(2)	4 920(2)	1 136(1)	Ru(8)	10 093(2)	6 895(2)	1 629(2)
Ru(4)	5 630(2)	4 918(2)	2 623(1)	Ru(9)	10 960(2)	7 160(2)	3 072(1)
Ru(5)	7 009(2)	4 288(2)	1 655(1)	Ru(10)	12 102(2)	7 811(1)	2 000(1)
C(1)	5 314(20)	4 099(16)	1 841(14)	C(2)	10 384(18)	7 879(15)	2 297(13)
P(1)	4 439(6)	2 826(5)	3 015(4)	P(3)	9 361(6)	9 259(5)	3 265(4)
C(111)	3 017(18)	2 982(9)	2 568(11)	C(311)	8 007(14)	8 929(10)	2 879(10)
C(112)	2 235(18)	2 435(9)	2 438(11)	C(312)	7 844(14)	8 187(10)	2 878(10)
C(113)	1 152(18)	2 598(9)	2 141(11)	C(313)	6 819(14)	7 900(10)	2 597(10)
C(114)	852(18)	3 309(9)	1 974(11)	C(314)	5 957(14)	8 355(10)	2 317(10)
C(115)	1 634(18)	3 856(9)	2 104(11)	C(315)	6 120(14)	9 097(10)	2 318(10)
C(116)	2 717(18)	3 693(9)	2 401(11)	C(316)	7 145(14)	9 384(10)	2 599(10)
C(121)	4 282(11)	2 902(11)	3 993(10)	C(321)	9 255(12)	9 418(11)	4 242(10)
C(122)	3 245(11)	2 969(11)	4 225(10)	C(322)	8 220(12)	9 485(11)	4 476(10)
C(123)	3 148(11)	2 966(11)	4 972(10)	C(323)	8 139(12)	9 675(11)	5 201(10)
C(124)	4 089(11)	2 895(11)	5 487(10)	C(324)	9 094(12)	9 797(11)	5 691(10)
C(125)	5 126(11)	2 827(11)	5 255(10)	C(325)	10 130(12)	9 729(11)	5 456(10)
C(126)	5 223(11)	2 831(11)	4 508(10)	C(326)	10 211(12)	9 540(11)	4 732(10)
C(3)	4 616(23)	1 875(18)	2 924(16)	C(5)	9 364(23)	10 233(17)	2 992(17)
C(4)	5 768(21)	1 604(17)	3 235(16)	C(6)	10 502(23)	10 505(19)	3 225(17)
P(2)	6 789(6)	2 242(5)	2 873(4)	P(4)	11 635(6)	9 903(5)	3 036(4)
C(211)	8 056(17)	2 244(10)	3 536(10)	C(411)	12 773(14)	10 140(10)	3 757(11)
C(212)	8 849(17)	2 784(10)	3 538(10)	C(412)	12 855(14)	10 795(10)	4 129(11)
C(213)	9 849(17)	2 729(10)	3 999(10)	C(413)	13 787(14)	10 947(10)	4 629(11)
C(214)	10 055(17)	2 134(10)	4 458(10)	C(414)	14 638(14)	10 444(10)	4 757(11)
C(215)	9 263(17)	1 593(10)	4 455(10)	C(415)	14 557(14)	9 789(10)	4 385(11)
C(216)	8 263(17)	1 649(10)	3 994(10)	C(416)	13 624(14)	9 637(10)	3 885(11)
C(221)	7 251(14)	1 754(9)	2 104(10)	C(421)	12 116(12)	10 292(12)	2 230(11)
C(222)	8 206(14)	1 974(9)	1 827(10)	C(422)	11 393(12)	10 720(12)	1 766(11)
C(223)	8 562(14)	1 607(9)	1 241(10)	C(423)	11 755(12)	11 051(12)	1 161(11)
C(224)	7 963(14)	1 020(9)	931(10)	C(424)	12 841(12)	10 954(12)	1 020(11)
C(225)	7 007(14)	799(9)	1 207(10)	C(425)	13 654(12)	10 525(12)	1 485(11)
C(226)	6 651(14)	1 167(9)	1 793(10)	C(426)	13 201(12)	10 194(12)	2 090(11)
C(11)	6 566(24)	3 796(19)	3 483(17)	C(61)	11 563(24)	8 414(20)	3 834(17)
O(11)	7 016(18)	3 955(14)	4 056(12)	O(61)	12 008(17)	8 328(14)	4 429(12)
C(21)	5 776(25)	2 821(20)	380(18)	C(71)	10 595(24)	9 130(20)	672(16)
O(21)	6 209(22)	2 437(17)	3(15)	O(71)	10 907(20)	9 536(15)	250(14)
C(22)	3 760(23)	3 071(17)	812(15)	C(72)	8 635(33)	8 760(25)	1 136(21)
O(22)	2 897(19)	2 823(15)	630(13)	O(72)	7 732(22)	8 945(16)	981(14)
C(23)	4 866(23)	4 180(19)	187(16)	C(73)	9 899(28)	7 744(22)	571(21)
O(23)	4 694(15)	4 297(12)	−426(11)	O(73)	9 686(18)	7 545(14)	−13(15)
C(31)	5 006(27)	5 668(21)	478(19)	C(81)	10 147(26)	6 231(20)	942(19)
O(31)	5 136(24)	6 153(18)	112(18)	O(81)	10 201(19)	5 811(14)	478(13)
C(32)	3 382(33)	4 999(26)	991(21)	C(82)	8 670(28)	6 750(21)	1 685(18)
O(32)	2 394(19)	5 028(14)	895(12)	O(82)	7 785(27)	6 540(19)	1 772(17)
C(41)	6 686(32)	5 506(24)	3 292(23)	C(91)	9 850(26)	6 897(20)	3 588(18)
O(41)	7 246(27)	5 729(20)	3 719(18)	O(91)	9 112(20)	6 676(15)	3 898(13)
C(42)	4 496(24)	5 127(18)	3 184(17)	C(92)	11 996(22)	6 820(16)	3 788(15)
O(42)	3 789(19)	5 118(15)	3 561(13)	O(92)	12 708(20)	6 569(15)	4 235(14)
C(43)	5 174(30)	5 761(22)	2 013(20)	C(93)	10 784(27)	6 281(21)	2 481(19)
O(43)	5 074(18)	6 382(13)	1 967(12)	O(93)	11 024(20)	5 656(15)	2 532(13)
C(51)	7 116(22)	5 064(17)	973(15)	C(101)	12 332(23)	7 024(17)	1 378(16)
O(51)	7 451(17)	5 484(13)	623(12)	O(101)	12 551(18)	6 616(14)	950(13)
C(52)	7 729(21)	3 666(16)	1 030(14)	C(102)	12 749(25)	8 450(21)	1 364(17)
O(52)	8 296(16)	3 341(13)	714(11)	O(102)	13 186(19)	8 823(15)	981(13)
C(53)	8 144(27)	4 727(21)	2 347(18)	C(103)	13 269(20)	7 546(15)	2 644(14)
O(53)	8 837(18)	4 925(15)	2 749(12)	O(103)	14 076(19)	7 336(14)	3 057(12)

days in the presence of PPh_3, conversion into (3b) was complete (Found: C, 45.8; H, 3.4; P, 4.0. Calc. for $C_{51}H_{30}O_{13}P_2Ru_5$: C, 42.7; H, 2.1; P, 4.1%).

(*b*) *With* $PMePh_2$. On addition of 1 equivalent of $PMePh_2$ to a solution of (1) in CH_2Cl_2 the monosubstituted product $[Ru_5C(CO)_{14}(PMePh_2)]$ (4a) may be isolated. On reaction with an excess of the phosphine the disubstituted product $[Ru_5C(CO)_{13}(PMePh_2)_2]$ (4b) and a further product $[Ru_5C(CO)_{12}(PMePh_2)_3]$ (4c) are quickly formed. The three products may be separated by t.l.c. in 50% diethyl ether–hexane (Found: C, 45.0; H, 3.7; P, 5.8. Calc. for $C_{52}H_{39}O_{12}P_3Ru_5$: C, 43.0; H, 2.7; P, 6.4%). ^{3}H.N.m.r.: (24 °C) −122.45 and −123.89 (relative intensity 2.09; (−70 °C) −120.09, −122.06, and −124.34 p.p.m. (relative intensity 1 : 1 : 1). Mass spectrum: highest mass *m*/*e* 1 453; $[Ru_5C(CO)_{12}(PMePh_2)_3]$.

(*c*) *With* $Ph_2P(CH_2)_2PPh_2$. Addition of 1 equivalent of the diphosphine to a solution of (1) in CH_2Cl_2 yielded the purple complex $[Ru_5C(CO)_{13}\{Ph_2P(CH_2)_2PPh_2\}]$ (6). Purification of

(6) was achieved by t.l.c. in 30% chloroform–hexane (Found: C, 40.4; H, 2.8; P, 4.8. Calc. for $C_{40}H_{24}O_{13}P_2Ru_5$: C, 37.5; H, 1.85; P, 4.8%). N.m.r.: (24 °C) δ −99.86; (−90 °C) −99.80 p.p.m.

(*d*) *With* X^-. Addition of 1 equivalent of the $[N(PPh_3)_2]^+$ NBu_4^+, or NMe_4^+ salt of F^-, Cl^-, Br^-, or I^- to a solution of (1) in CH_2Cl_2 resulted in a change in colour of the solution from red to yellow due to the formation of the salt $[Ru_5C(CO)_{15}X]^-$ (X = F, Cl, Br, or I). Protonation of these species to give the complexes $[Ru_5H(C)(CO)_{15}X]$ was achieved by direct addition of concentrated H_2SO_4 to the CH_2Cl_2 solution.

(*e*) *With* HCl. A steady stream of HCl gas was bubbled through a stirred solution of (1) (20 mg) in CH_2Cl_2 (20 cm^3) for 30 s. The yellow solution was then evaporated to dryness, giving a yellow solid, $[Ru_5H(C)(CO)_{15}Cl]$ (9a) (20.5 mg, 98.5%) (Found: C, 20.9; H, 0.95; Cl, 3.85. Calc. for $C_{16}HClO_{15}Ru_5$: C, 19.7; H, 0.01; Cl, 3.65%). ^1H N.m.r.: (24—80 °C) δ 22.1 p.p.m. Mass spectrum: highest mass *m*/*e* 946, $[Ru_5H(C)(CO)_{14}Cl]$; lowest mass *m*/*e* 517, Ru_5C.

(*f*) *With* HBr. The reaction of (1) with HBr was carried out in the same way as with HCl (see above) giving $[Ru_5H(CO)(CO)_{15}Br]$ (10a) (Found: C, 18.2; H, 0.45. Calc. for $C_{16}HBrO_{15}Ru_5$: C, 18.8; H, 0.00%). ^1H N.m.r.: (24—80 °C) δ −22.1 p.p.m. Mass spectrum: highest mass *m*/*e* 1 099, $[Ru_5H_2(C)(CO)_{15}Br_2]$; lowest mass *m*/*e* 517, Ru_5C.

After stirring (10a) for 10 h in CH_2Cl_2 with proton sponge the anion (10) was regenerated.

(*g*) *With* Cl_2. Chlorine gas was bubbled slowly through a solution of (1) in CH_2Cl_2 for about 3 min. The yellow solution was evaporated to dryness by N_2 flow to give a yellow solid having the same i.r. spectrum as $[Ru_2(CO)_6Cl_4]$. The reaction was repeated but with a slow addition of a solution of Cl_2 in CH_2Cl_2 and no intermediate products were detected (Found: C, 14.2; Cl, 25.9. Calc. for $C_6Cl_4O_6Ru_2$: C, 14.1; Cl, 27.7%). Mass spectrum: highest mass *m*/*e* 512, $[Ru_2(CO)_6Cl_4]$.

(*h*) *With* I_2. Addition of 1 equivalent of a solution of I_2 in cyclohexane to a solution of (1) in CH_2Cl_2 gave a brown solution. Evaporation by N_2 flow then gave a solid, $[Ru_5C(CO)_{15}I_2]$ (14) (Found: C, 20.8; I, 22.7. Calc. for $C_{16}I_2O_{15}Ru_5$: C, 16.1; I, 21.3%). Mass spectrum: highest mass *m*/*e* 1 163, $[Ru_5C(CO)_{15}I_2]$; lowest mass *m*/*e* 517, Ru_5C.

(*i*) *With* MeCN. A suspension of $[Ru_5C(CO)_{15}]$ (10 mg) in acetonitrile (10 cm^3) was stirred under an atmosphere of N_2 for about 5 min. The red crystals dissolved slowly to give an orange solution. Evaporating the solvent by fast N_2 stream gave orange crystals of $[Ru_5C(CO)_{15}(MeCN)]$ (2) which when dissolved in dichloromethane or when placed under vacuum for 14 h regenerated $[Ru_5C(CO)_{15}]$.

Pyrolysis of $[Ru_5C(CO)_{15}]$ *under Argon.*—After heating a solution of $[Ru_5C(CO)_{15}]$ (30 mg) in heptane (50 cm^3) to 200 °C under 10 atm Ar for 4 h an orange solution containing a fine suspension of dark coloured particles was produced. Filtration followed by evaporation of the solution to dryness yielded $[Ru_6C(CO)_{17}]$ (17.2 mg, 59%). The dark solid was extracted with acetone giving a soluble anionic product (6 mg, 20%) and leaving ruthenium metal (6 mg, 20%).

Reaction of $[Ru_5C(CO)_{13}\{Ph_2P(CH_2)_2PPh_2\}]$ *with* H_2.—On treatment of $[Ru_5C(CO)_{13}\{Ph_2P(CH_2)_2PPh_2\}]$ (6) with H_2 (50 atm, 90 °C, 1.5 h) in heptane (50 cm^3) an orange solution was produced. Evaporation by N_2 flow followed by t.l.c. in 50% chloroform–hexane yielded $[Ru_5H_2(C)(CO)_{12}\{Ph_2P(CH_2)_2PPh_2\}]$ (7) (orange, R_f 0.5, 70%) and at least three minor products (pink, R_f 0.8, 5%; yellow, R_f 0.75, 5%; purple, R_f 0.35, 1%), and some unreacted (6) (purple, R_f 0.6, 10%). The major product (7) was purified by t.l.c. in 30% chloroform–hexane. N.m.r.: ^{31}P, −79.2, and −86.6, ^1H, −13.83, −13.87, −13.88, −13.91, −19.90, −19.92, −19.97, and −19.94 p.p.m. (relative intensity 1 : 1 : 1 : 1 : 1 : 1 : 1 : 1).

Further reaction of (7) with H_2 (50 atm, 140 °C, 1 h) in heptane gave an orange-brown solution which when evaporated to dryness and separated by t.l.c. in 50% chloroform–hexane was shown to contain the pink (20%) and yellow (80%) minor products of the previous reaction.

Molecular Structure Determinations.—Single crystals of (1), (2), (3a), (3b), and (7) were mounted on glass fibres, and after initial photographic investigations were transferred to four-circle diffractometers upon which intensity data were recorded. Details of crystal parameters, data-collection parameters, and refinement data are summarised in Table 5.

All the data sets were corrected for Lorentz polarization factors. Neutral-atom scattering factors were employed throughout.[20] The structures were solved using programs written by Professor G. M. Sheldrick.[21] All computations for structure (1) were carried out on the computer at the Polytechnic of North London. The computations for (3a) were carried out on the ECLIPSE computer at the University of Göttingen, and for this structure data reduction included online profile fitting of *X*-ray data.[22] The other three structures were solved on the IBM 370/165 at the University of Cambridge.

In the structure of (1) the Ru atoms were assigned anisotropic thermal parameters during refinement. In (2) the Ru, O, and N atoms were assigned anisotropic thermal parameters, and the methyl H atoms were included with the C–H distances fixed at 1.08 Å; the H atoms were assigned a common isotropic thermal parameter. In (3a) all the non-hydrogen atoms were assigned anisotropic thermal parameters and the H atoms were constrained to ride 0.96 Å from the relevant C atom. In (3b) the Ru, O, and P atoms were refined anisotropically, while in (7) only the Ru and P atoms were refined anisotropically. In both these structures the phenyl rings were refined as rigid bodies with C–H fixed at 1.08 Å. In (7) the CH_2 hydrogen atoms were also constrained to ride in idealised positions.

The final atomic co-ordinates for (1), (2), (3a), (3b), and (7) are presented in Tables 6—10, respectively.

Acknowledgements

We thank the S.E.R.C. for financial support.

References

1 R. Pettit, 2nd International Symposium on Homogeneous Catalysis, Dusseldorf, 1980.
2 B. F. G. Johnson, J. Lewis, and I. G. Williams, *J. Chem. Soc. A*, 1970, 901; C. R. Eady, B. F. G. Johnson, and J. Lewis, *J. Chem. Soc., Dalton Trans.*, 1975, 2606.
3 A. Sirigu, M. Bianchi, and E. Benedetti, *Chem. Commun.*, 1969, 596.
4 R. Mason and W. R. Robinson, *Chem. Commun.*, 1968, 468.
5 D. H. Farrar, P. F. Jackson, B. F. G. Johnson, J. Lewis, J. N. Nicholls, and M. McPartlin, *J. Chem. Soc., Chem. Commun.*, 1981, 415.
6 C. R. Eady, B. F. G. Johnson, J. Lewis, and T. Matherson, *J. Organomet. Chem.*, 1973, **57**, C82.
7 E. H. Braye, L F. Dahl, W. Hübel, and D. L. Wampler, *J. Am. Chem Soc.*, 1962, **84**, 4633.
8 P. F. Jackson, B. F. G. Johnson, J. Lewis, J. N. Nicholls, M. McPartlin, and W. J. H. Nelson, *J. Chem. Soc., Chem. Commun.*, 1980, 564.
9 K. Wade, *Adv. Inorg. Chem. Radiochem.*, 1976, **18**, 1; C. R.

Eady, B. F. G. Johnson, and J. Lewis, *J. Chem. Soc., Dalton Trans.*, 1975, 2606.

10 J. M. Fernandez, B. F. G. Johnson, J. Lewis, and P. R. Raithby, *J. Chem. Soc., Dalton Trans.*, 1981, 2250.

11 E. M. Holt, K. H. Whitmire, and D. F. Schriver, *J. Organomet. Chem.*, 1981, **213**, 125; J. H. Jones, M. A. Beno, J. M. Williams, J. Zimmie, M. Tachikawa, and E. L. Muetterties, *Proc. Natl. Acad. Sci. USA*, 1981, **78**, 668.

12 B. F. G. Johnson, J. Lewis, B. E. Reichert, K. T. Schorpp, and G. M. Sheldrick, *J. Chem. Soc., Dalton Trans.*, 1977, 1417.

13 G. R. Steinnetz, A. D. Harley, and G. L. Geoffroy, *Inorg. Chem.*, 1980, **19**, 2985.

14 A. J. Carty, S. A. MacLaughlin, N. J. Taylor, and E. Sappa, *Inorg. Chem.*, 1981, **20**, 4437.

15 S. C. Brown, J. Evans, and M. Webster, *J. Chem. Soc., Dalton Trans.*, 1981, 2263.

16 E. J. Forbes, N. Goodhand, D. L. Jones, and T. A. Hamor, *J. Organomet. Chem.*, 1979, **182**, 143.

17 A. G. Orpen, *J. Chem. Soc., Dalton Trans.*, 1980, 2059.

18 M. R. Churchill and R. A. Lashewycz, *Inorg. Chem.*, 1978, **17**, 1950.

19 M. R. Churchill, R. A. Lashewycz, J. R. Shapley, and S. I. Richter, *Inorg. Chem.*, 1980, **19**, 1277.

20 'International Tables for *X*-Ray Crystallography,' Kynoch Press, Birmingham, 1974, vol. 4.

21 SHELX, crystal structure solving package, G. M. Sheldrick, Cambridge, 1976; SHELXTL Mini-computer crystal structure solving package, G. M. Sheldrick, Göttingen, 1980.

22 W. Clegg, *Acta Crystallogr., Sect. A*, 1981, **37**, 22.

Received 5th July 1982; *Paper* 2/1132